SUPPLEMENTARY APPENDIX

ATP11C is a major flippase in human erythrocytes and its defect causes congenital hemolytic anemia

Nobuto Arashiki,[1] Yuichi Takakuwa,[1] Narla Mohandas,[2] John Hale,[2] Kenichi Yoshida,[3] Hiromi Ogura,[4] Taiju Utsugisawa,[4] Shouichi Ohga,[5] Satoru Miyano,[6] Seishi Ogawa,[3] Seiji Kojima,[7] and Hitoshi Kanno,[4,8]

[1]Department of Biochemistry, School of Medicine, Tokyo Women's Medical University, Japan; [2]Red Cell Physiology Laboratory, New York Blood Center, NY, USA; [3]Department of Pathology and Tumor Biology, Graduate School of Medicine, Kyoto University, Japan; [4]Department of Transfusion Medicine and Cell Processing, School of Medicine, Tokyo Women's Medical University, Japan; [5]Department of Pediatrics, Graduate School of Medicine, Yamaguchi University, Japan; [6]Laboratory of DNA Information Analysis, Human Genome Center, Institute of Medical Science, The University of Tokyo, Japan; [7]Department of Pediatrics, Graduate School of Medicine, Nagoya University, Japan; and [8]Division of Genomic Medicine, Department of Advanced Biomedical Engineering and Science, Graduate School of Medicine, Tokyo Women's Medical University, Japan

 doi:10.3324/haematol.2016.142273

Received: January 13, 2016.

Accepted: February 26, 2016.

Pre-published: March 4, 2016.

Correspondence: kanno.hitoshi@twmu.ac.jp

Online Supplementary Information

Reagents, laboratory instruments, and compositon of buffer solutions used in this study.

D-glucose, N-ethylmaleimide (NEM), and sucrose were purchased from Wako Pure Chemical (Osaka, Japan). 1-palmitoyl-2-{6-[(7-nitro-2-1,3-benzoxadiazol-4-yl)amino]hexanoyl}-sn-glycero-3-phosphoser ine (NBD-PS) was purchased from Avanti Polar Lipids, Inc. (Alabaster, AL, USA). Percoll was purchased from GE Healthcare (Buckinghamshire, UK). Bovine serum albumin (BSA) and A23187 were purchased from Sigma-Aldrich, Inc. (St. Louis, MO, USA). Fluorescein isothiocyanate-conjugated Annexin V (FITC-Annexin V) was purchased from MBL International Corp. (Woburn, MA, USA). SureSelect Human All Exon V4 kit was purchased from Agilent Technologies (Santa Clara, CA, USA). HiSeq 2000 platform used for massively parallel sequencing was purchased from Illumina (San Diego, CA, USA). Flowcytometer (Cell Lab Quanta SC) was purchased from Beckman Coulter, Inc. (Brea, CA, USA). Phosphate-buffered saline with glucose (PBS-G) was composed of 137 mM NaCl, 8.1 mM Na_2HPO_4, 2.68 mM KCl, 1.47 mM KH_2PO_4, 10 mM D-glucose. Tris-buffered saline with glucose (TBS-G) was composed of 25 mM Tris-Cl (pH 7.4), 150 mM NaCl, 10 mM D-glucose.

Genotyping the Thr418Asn mutation by direct sequencing of ATP11C exon 13

Genomic DNA was extracted and purified from white blood cells using QIAamp DNA Blood Mini Kit (Qiagen, Hilden, Germany). Exon 13, including the coding region for p.Thr418, was amplified using the primers (forward, 5′-TGT GTC CTT GTT TTA GGT GG-3′; reverse, 5′-TGC ACC TTA TCT ACT TTG TC-3′) and KOD plus DNA polymerase (Toyobo, Osaka, Japan). PCR was performed for 40 cycles with annealing at 48 °C using GeneAmp PCR system 9700 (Applied Biosystems, Foster City, CA, USA). PCR products (183 bp) were separated by 1.5% agarose gel electrophoresis and extracted using a QIAquick DNA Extraction kit (Qiagen), and 4 ng purified PCR products was sequenced (Eurofins Genomics, Brussels, Belgium) using the reverse primer descried above for amplification of exon 13. Figure 1C displays the sequences of the antisense strand.

Methods for Online Supplementary Information

Analyses of enzyme and reduced glutathione, isopropanol test, and eosin 5′-maleimide binding test for erythrocytes

All enzyme assays were performed as previously described.[1,2] The reduced glutathione assay, isopropanol test, and eosin 5′-maleimide binding test were performed as previous described.[3-5]

Measurement of erythrocyte deformability

Whole blood obtained from the control, proband, and mother was suspended in Stractan (viscosity of 22 cP, 290 mOsm) and examined by an ektacytometer as previously described.[6] Briefly, the suspension was subjected to linearly increasing shear stress, and changes in laser diffraction patterns were analyzed to derive the deformability index (DI). The DI provides a measure of the ellipticity of deforming erythrocytes in the flow field. DI was measured as a function of applied shear stress up to 150 dynes/cm^2. The rate of increase in DI is a measure of membrane deformability, and the maximal DI value indicates the surface area of erythrocytes.

Analyses of erythrocyte membrane proteins and lipids

Washed erythrocytes were lysed and washed three times in 5 mM phosphate buffer at 4 °C to prepare membrane ghosts. Protein concentration was measured by the Bradford method using Coomassie Plus Protein Assay Reagent (Thermo Scientific, Rockford, IL, USA). Membrane proteins (8 μg/lane) were separated by SDS-PAGE using an 8% acrylamide gel followed by Coomassie brilliant blue staining. Membrane lipids were extracted from 40 μg membrane ghosts with 5.5 volumes isopropanol and 3.5 volumes chloroform. After centrifugation to remove aggregated proteins, the supernatant was transferred to another tube and completely evaporated. The residue was dissolved in 2 mL CM solution (2:1 chloroform:methanol), and 400 μL 50 mM KCl was added to remove hydrophilic substances (Folch partition method).[7] After vigorous shaking, the organic bottom layer was transferred to another tube and completely evaporated. The purified membrane lipids were dissolved in 30 μL chloroform and then spotted onto a silica gel plate (HPTLC plate Silica gel 60; Merck, Darmstadt, Germany). Plates were developed with hydrophobic solution (65:25:5 chloroform:methanol:ammonia solution (28%))[8] and stained with iodine. Lipid species corresponding to each visualized band were identified by comparison with the bands obtained using pure lipid standards and NBD-labeled lipids (purchased from Avanti Polar Lipids, Inc.).

RNAseq analyses for human and mouse erythroblasts.

Human and murine purified erythroblasts at distinct stages of terminal differentiation generated from CD34+ cells were prepared and RNAseq analyses were performed as previously described.[9]

References for Online Supplementary Information

1. Beutler E, Blume KG, Kaplan JC, Löhr GW, Ramot B, Valentine WN. International

Committee for Standardization in Haematology: recommended methods for red cell enzyme analysis. Br J Haematol. 1977;35(2):331-340.

2. Beutler E. *Red cell metabolism–A Manual of biochemical methods 3rd edition.* Grune & Stratton, Inc., New York, NY, USA. 1984.
3. Beutler E, Duron O, Nelly B. Improved methods for determination of blood glutathione. J Lab Clin Med. 1963;61:882–890.
4. Carrell RW, Kay R. A simple method for the detection of unstable haemoglobins. Br J Haematol. 1972;23(5):615-619.
5. King MJ, Behrens J, Rogers C, Flynn C, Greenwood D, Chambers K. Rapid flow cytometric test for the diagnosis of membrane cytoskeleton-associated haemolytic anaemia. Br J Haematol. 2000;111(3):924-933.
6. Manno S, Takakuwa Y, Mohandas N. Identification of a functional role for lipid asymmetry in biological membranes: Phosphatidylserine-skeletal protein interactions modulate membrane stability. Proc Natl Acad Sci U S A. 2002;99(4):1943-1948.
7. Folch J, Lees M, Sloane Stanley GH. A simple method for the isolation and purification of total lipides from animal tissues. J Biol Chem. 1957;226(1):497-509.
8. Kinsey WH, Decker GL, Lennarz WJ. Isolation and partial characterization of the plasma membrane of the sea urchin egg. J Cell Biol. 1980;87(1):248-254.
9. An X, Schulz VP, Li J, et al. Global transcriptome analyses of human and murine terminal erythroid differentiation. Blood. 2014;123(22):3466-3477.

Supplementary Tables

Supplementary Table S1. **Erythrocyte enzyme assay, reduced glutathione, isopropanol test, and eosin 5′-maleimide binding test.**

	Normal range (mean±SD)	Control	Proband
Hexokinase (Hx)	1.08-1.46	1.70	1.80
Glucosephosphate isomerase (GPI)	57.2-70.3	72.1	57.9
Phosphofructokinase (PFK)	14.1-20.0	20.7	20.5
Aldolase (ALD)	2.62-6.30	7.47	9.98
Triosephosphate isomerase (TPI)	1052-1567	1775	1610
Glyceraldehyde-3-phosphate dehydrogenase (GA3PD)	235-294	373	366
Phosphoglycerate kinase (PGK)	264-326	452	357
Monophosphoglyceromutase (MPGM)	15.7-23.2	20.9	20.4
Enolase (ENOL)	3.89-6.30	7.19	6.49
Pyruvate kinase (PK)	13.0-19.8	23.0	26.1
PK Low S (%)	14.8-28.4	16.8	14.9
Lactate dehydrogenase (LDH)	145-188	264	214
Glucose-6-phosphate dehydrogenase (G6PD)	7.61-9.81	10.55	11.12
6-Phosphogluconate dehydrogenase (6PGD)	9.00-10.7	13.59	9.92
Glutathione reductase (GR)	4.08-8.42	7.73	6.21
GR + FAD	6.62-10.3	12.1	11.5
Glutathione peroxidase (GSH-Px)	37.2-51.4	58.7	47.5
Adenylate kinase (AK)	165-307	330	410
Adenosine deaminase (ADA)	0.87-1.59	1.52	1.27
Acetylcholinesterase (Ach-E)	28.6-42.7	39.3	37.5
Pyrimidine 5'-nucleotidase (P5N) (CMPase)*	6.90-10.8	9.83	13.64
Pyrimidine 5'-nucleotidase (P5N) (UMPase)*	9.75-15.5	14.6	21.5
Reduced glutathione (GSH)**	65.9-88.5	82.6	76.8
Isopropanol test	(-)	(-)	(-)
Binding of eosin 5'-maleimide***	46.6-57.5	46.6	46.8

Units for each test are IU/gHb, *μmol Pi liberated/h/gHb, **mg/dL RBC, ***mean channel fluorescence.

Supplementary Table S2. **Single nucleotide variants and Indels revealed from whole-exome sequencing for proband's genome.** Fifty-four non-synonymous single nucleotide variants (SNVs) focused from 303 SNVs on the evolutional conservation and the malignant potential and 46 Indels were listed by alphabetical order of the gene name, respectively. Nucleotide ID was indicated as a GenBank Accession Number.

Gene	Function	Exonic Funcion	Nucleotide ID:Nucleotide:Amino acid substitutions
54 non-synonymous SNVs			
ATP11C	exonic	nonsynonymous SNV	NM_001010986:c.C1253A:p.T418N
AUTS2	exonic	nonsynonymous SNV	NM_001127231:c.C188A:p.P63Q
C3orf62	exonic	nonsynonymous SNV	NM_198562:c.G413A:p.G138E
CCDC24	exonic	nonsynonymous SNV	NM_152499:c.C611G:p.P204R
CFTR	exonic	nonsynonymous SNV	NM_000492:c.A113G:p.Y38C
CGN	exonic	nonsynonymous SNV	NM_020770:c.C106T:p.R36C
DAPK3	exonic	nonsynonymous SNV	NM_001348:c.C91T:p.R31W
DEFB132	exonic	nonsynonymous SNV	NM_207469:c.T20C:p.V7A
DNAH8	exonic	nonsynonymous SNV	NM_001206927:c.C11837A:p.P3946H
FBXL4	exonic	nonsynonymous SNV	NM_012160:c.C61T:p.R21C
GFM1	exonic	nonsynonymous SNV	NM_024996:c.C170A:p.S57Y
GNPAT	exonic	nonsynonymous SNV	NM_014236:c.C953T:p.S318F
GRIN3A	exonic	nonsynonymous SNV	NM_133445:c.G3247C:p.E1083Q
HSPBP1	exonic	nonsynonymous SNV	NM_012267:c.C92G:p.S31C
IFI16	exonic	nonsynonymous SNV	NM_001206567:c.A84C:p.L28F
IKBKAP	exonic	nonsynonymous SNV	NM_003640:c.G898A:p.V300M
ITGA3	exonic	nonsynonymous SNV	NM_002204:c.G490T:p.V164L
KAT6A	exonic	nonsynonymous SNV	NM_006766:c.G4484A:p.R1495H
KDM6B	exonic	nonsynonymous SNV	NM_001080424:c.C1532A:p.P511H
KIF20B	exonic	nonsynonymous SNV	NM_016195:c.A2146G:p.N716D
LRRC47	exonic	nonsynonymous SNV	NM_020710:c.C1112T:p.T371M
MAMDC4	exonic	nonsynonymous SNV	NM_206920:c.G2530A:p.G844R
MAN2A2	exonic	nonsynonymous SNV	NM_006122:c.T505G:p.F169V
MAPT	exonic	nonsynonymous SNV	NM_016834:c.G643A:p.G215R
MOXD1	exonic	nonsynonymous SNV	NM_015529:c.C1361A:p.T454N
MPHOSPH10	exonic	nonsynonymous SNV	NM_005791:c.G1525A:p.A509T
NBAS	exonic	nonsynonymous SNV	NM_015909:c.C4951T:p.L1651F
NECAB3	exonic	nonsynonymous SNV	NM_031232:c.C1105T:p.R369C
NOTCH1	exonic	nonsynonymous SNV	NM_017617:c.C6351A:p.N2117K
OR2L3	exonic	nonsynonymous SNV	NM_001004687:c.C707T:p.A236V
OR4F15	exonic	nonsynonymous SNV	NM_001001674:c.C59T:p.S20L
PABPC1L	exonic	nonsynonymous SNV	NM_001124756:c.C1297T:p.P433S
PCDHGA1	exonic	nonsynonymous SNV	NM_018912:c.G1796T:p.G599V
PKD1L2	exonic	nonsynonymous SNV	NM_001076780:c.T1820C:p.V607A
PLCG2	exonic	nonsynonymous SNV	NM_002661:c.A1430C:p.Q477P
POLR1B	exonic	nonsynonymous SNV	NM_001137604:c.C803T:p.A268V
PTCH2	exonic	nonsynonymous SNV	NM_001166292:c.G2842A:p.G948S
PTGES2	exonic	nonsynonymous SNV	NM_025072:c.C1072T:p.H358Y
RPS6KA5	exonic	nonsynonymous SNV	NM_004755:c.C1465T:p.H489Y
SASH1	exonic	nonsynonymous SNV	NM_015278:c.G239A:p.R80K

SEMA4G	exonic	nonsynonymous SNV	NM_001203244:c.G218A:p.R73Q
SEPHS1	exonic	nonsynonymous SNV	NM_001195602:c.C599T:p.T200M
SHANK1	exonic	nonsynonymous SNV	NM_016148:c.C1361T:p.P454L
SON	exonic	nonsynonymous SNV	NM_032195:c.T2222C:p.M741T
SYPL2	exonic	nonsynonymous SNV	NM_001040709:c.G343A:p.A115T
TCIRG1	exonic	nonsynonymous SNV	NM_006019:c.G154C:p.V52L
TCTN1	exonic	nonsynonymous SNV	NM_001082537:c.T768G:p.C256W
TEAD4	exonic	nonsynonymous SNV	NM_003213:c.G166A:p.A56T
TEX2	exonic	nonsynonymous SNV	NM_018469:c.T3233C:p.L1078S
TRPM8	exonic	nonsynonymous SNV	NM_024080:c.G1424A:p.R475H
VEGFC	exonic	nonsynonymous SNV	NM_005429:c.T1256G:p.M419R
VTN	exonic	nonsynonymous SNV	NM_000638:c.G1050T:p.M350I
ZC3HAV1	exonic	nonsynonymous SNV	NM_020119:c.A745C:p.S249R
ZNF248	exonic	nonsynonymous SNV	NM_021045:c.A178G:p.I60V
46 Indels			
ACVR1B	exonic	frameshift insertion	NM_004302:c.66_67insG:p.G22fs
ADAMTS2	exonic	nonframeshift insertion	NM_014244:c.71_72insTGC:p.P24delinsLP
AGAP6	exonic	frameshift deletion	NM_001077665:c.1541delC:p.S514fs
ALMS1	exonic	nonframeshift insertion	NM_015120:c.35_36insGGA:p.L12delinsLE
ALOX5AP	splicing		(NM_001204406:exon1:c.116+1->TA)
ALOX5AP	exonic	frameshift insertion	NM_001204406:c.116_117insGTGT:p.W39fs
APOA1BP	exonic	nonframeshift deletion	NM_144772:c.165_167del:p.55_56del
AR	exonic	nonframeshift deletion	NM_000044:c.171_173del:p.57_58del
ASCL1	exonic	nonframeshift insertion	NM_004316:c.149_150insGCA:p.A50delinsAQ
C11orf80	exonic	nonframeshift insertion	NM_024650:c.77_78insGGC:p.G26delinsGA
C12orf56	exonic	nonframeshift insertion	NM_001170633:c.703_704insAAC:p.S235delinsNS
CASKIN1	exonic	nonframeshift deletion	NM_020764:c.3831_3833del:p.1277_1278del
CASKIN2	exonic	frameshift deletion	NM_001142643:c.1936delC:p.Q646fs
CCDC66	splicing		
CCNT1	splicing		(NM_001240:exon7:c.497-2->T)
COX8C	exonic	frameshift insertion	NM_182971:c.144_145insG:p.L48fs
CPEB2	exonic	nonframeshift insertion	NM_001177381:c.627_628insCCG:p.S209delinsSP
CYTH3	splicing		(NM_004227:exon3:c.117+2T>-)
DNAJC27	exonic	nonframeshift deletion	NM_001198559:c.233_235del:p.78_79del
DNM2	exonic	nonframeshift deletion	NM_001005362:c.2397_2399del:p.799_800del
FAM48B1	exonic	nonframeshift deletion	NM_001136234:c.1494_1496del:p.498_499del
FOXO3	exonic	frameshift deletion	NM_001455:c.534_535del:p.178_179del
GP1BA	exonic	frameshift deletion	NM_000173:c.1285delG:p.E429fs
HCRTR1	splicing		
HTT	exonic	nonframeshift deletion	NM_002111:c.52_54del:p.18_18del
IST1	exonic	frameshift insertion	NM_014761:c.710_711insA:p.P237fs
LFNG	exonic	frameshift deletion	NM_001166355:c.135_138del:p.45_46del
LPCAT3	exonic	frameshift deletion	NM_005768:c.1419_1420del:p.473_474del
LRP5	exonic	nonframeshift insertion	NM_002335:c.32_33insGCT:p.P11delinsPL
MDGA1	exonic	frameshift insertion	NM_153487:c.815_816insC:p.Q272fs
MRGPRF	exonic	frameshift deletion	NM_001098515:c.565delG:p.A189fs
MUC22	exonic	frameshift deletion	NM_001198815:c.1907delC:p.T636fs
OTUD7A	exonic	nonframeshift deletion	NM_130901:c.2065_2067del:p.689_689del
RBM5	exonic	frameshift deletion	NM_005778:c.2447_2448del:p.816_816del

SNX19	exonic	frameshift deletion	NM_014758:c.2857delT:p.Y953fs
SYNGR1	exonic	nonframeshift insertion	NM_004711:c.607_608insACC:p.T203delinsNP
TAF1B	exonic	frameshift deletion	NM_005680:c.187delA:p.K63fs
TAPT1	exonic	frameshift insertion	NM_153365:c.1669_1670insA:p.D557fs
TCP11	exonic	frameshift deletion	NM_001093728:c.17delG:p.G6fs
TMEM176B	splicing		
WNK1	exonic	frameshift insertion	NM_213655:c.2172_2173insC:p.V724fs
ZFHX4	exonic	nonframeshift deletion	NM_024721:c.4768_4770del:p.1590_1590del
ZNF230	exonic	frameshift deletion	NM_006300:c.451delG:p.D151fs
ZNF528	splicing		
ZNF598	exonic	nonframeshift deletion	NM_178167:c.1665_1667del:p.555_556del
ZNF718	exonic	frameshift deletion	NM_001039127:c.479_483del:p.160_161del

Abbreviations used are del; deletion, ins; insertion, fs; frame shift.

Figure legends for Online Supplementary Information

Supplementary Figure S1. **Analyses of erythrocyte deformability and membrane proteins and lipids.** (A) Measurement of erythrocyte deformability using an ektacytometer. Black, red, and green indicate the control, proband, and maternal samples, respectively. No differences were observed in erythrocyte deformability. DI, deformability index. (B) SDS-PAGE analysis of membrane proteins from control, proband, and maternal erythrocytes. Membrane ghosts (8 μg protein/lane) were separated electrophoretically on an 8% acrylamide gel and stained with Coomassie brilliant blue (CBB). No differences in amounts or migration patterns are observed for major membrane proteins. (C) Thin layer chromatography for lipids extracted from normal, proband, and maternal erythrocyte membranes (40 μg protein each). Membrane lipids dissolved in chloroform were spotted (*arrow head*), developed by hydrophobic solution, and stained with iodine. Lipid species corresponding to each band were determined by comparison with commercial pure lipid standards and NBD-labeled lipids (data not shown). PA; phosphatidic acid, SM; sphingomyelin, PC; phosphatidylcholine, PE; phosphatidylethanolamine. No difference in lipid content was observed.

Supplementary Figure S2. **Flipping activity of PS in NEM-treated erythrocytes.** Primary NBD-derived fluorescence data from flow cytometry for the experiments using NEM-treated erythrocytes as described in Figure 2. No flipped NBD-PS was observed after 20 min in any of the three erythrocyte samples, indicating that NEM effectively prevented flipping activity.

Supplementary Figure S3. **mRNA levels of flippase genes in human and mouse erythroblasts.** RNAseq analyses were performed for flippase genes, *ATP8A1*, *8A2*, *11A*, and *11C*, in human (A) and mouse (B) erythroblasts at distinct stages of terminal erythroid differentiation. RNA expression levels were indicated as fragments per kilobase per million mapped fragments (FPKM). Pro; proerythroblast, (E, L)Baso; (early, late) basophilic erythroblast, Poly; polychromatophilic erythroblast, Ortho; orthochromatophilic erythroblast.

Supplementary Figure S1

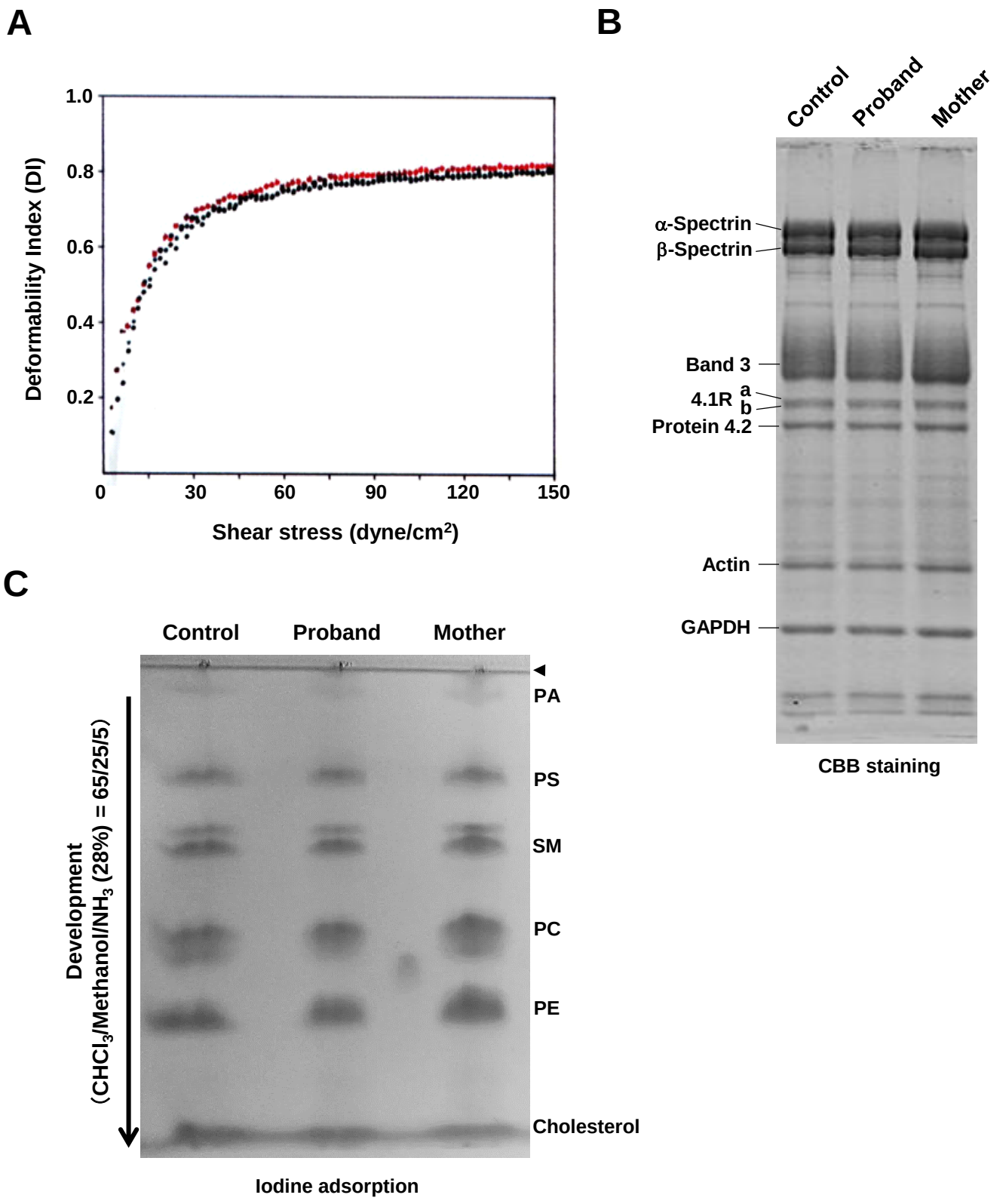

Supplementary Figure S2

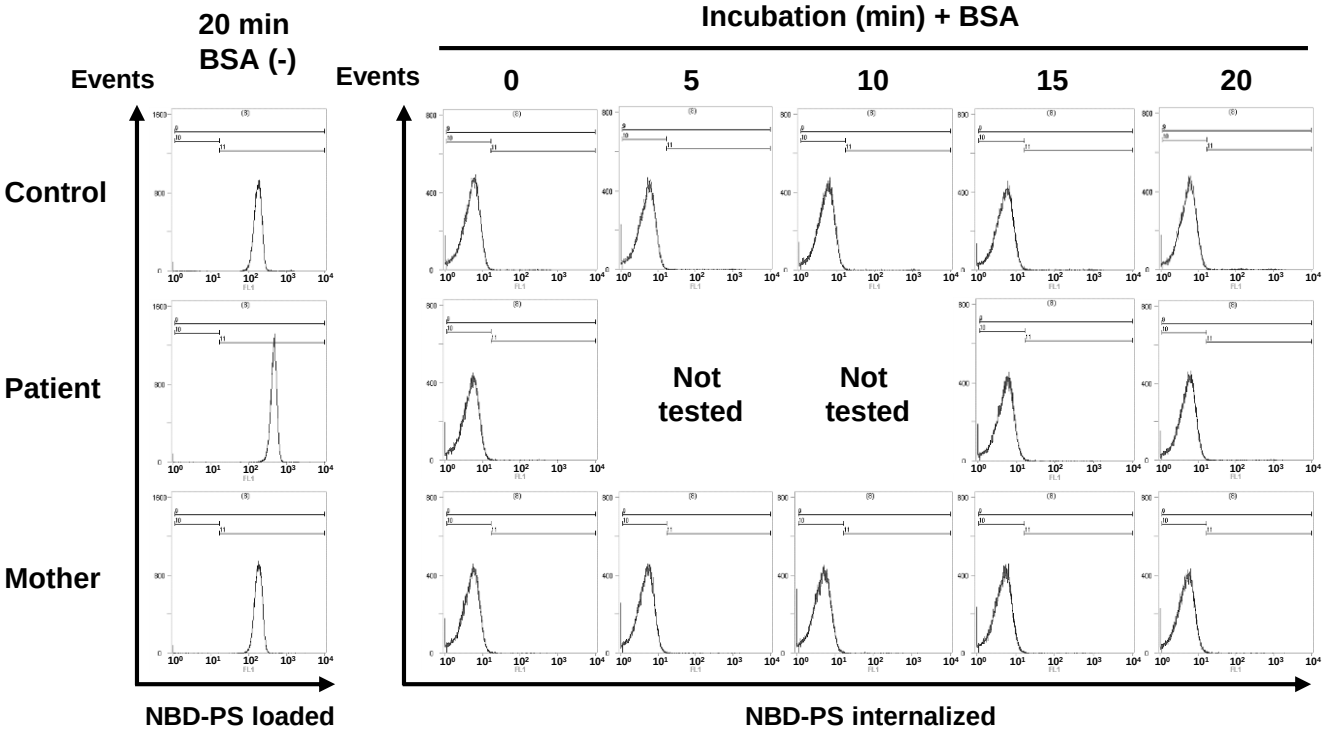

Supplementary Figure S3

A

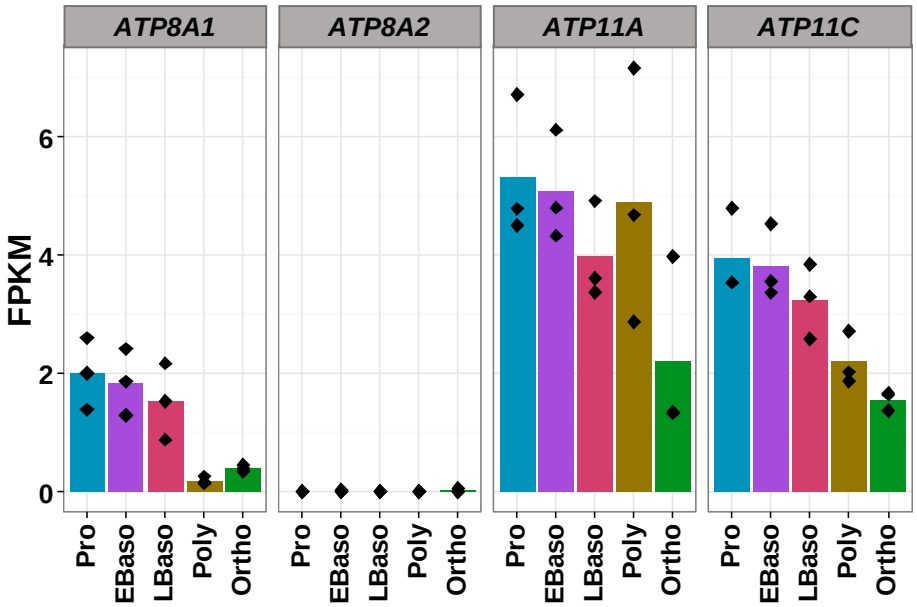

B